Analytical Model for Comb Capacitance Fringe Fields

Hanno Hammer

***Abstract*—Analytical expressions for electric potential and electric fringe fields in regions above the fingers of MEMS (Micro-Electro-Mechanical-System) comb capacitances are derived using potential-theoretic methods. The formulae are valid for 1) a comb geometry exhibiting a large number of identical fingers and 2) a finger geometry where the gap between fingers is small compared to height of fingers and finger overlap. For these conditions, symmetries inherent to the comb geometry can be exploited fruitfully to set up a properly defined Dirichlet problem formulation for the potential which can be solved for explicitly, yielding a series expansion for electrostatic potential and electric field components. The accuracy of approximated analytical solutions, obtained by truncating the series expansions to contain only a finite number of terms, is compared with results obtained from Finite Element simulations of electrostatic potential and electric field. From the analytic result, an approximation to the levitation force acting on the upper finger surfaces is derived. A formula expressing the mean length of fringe electric field lines emanating from upper finger surfaces into the ambient space is presented.**

***Index Terms*—Comb capacitance, electric field, fringe field, in-plane interdigitated comb drive, levitation effect, length of electric field lines.**

I. Introduction

ELECTROSTATIC comb capacitances are some of the most ubiquitous components used in microelectromechanical (MEMS) devices containing movable mechanical structures for either electrostatic actuation or capacitive sensing. Comb capacitances essentially exist in two varieties: (1) as in-plane interdigitated combs, often featuring symmetrically shaped fingers on both the static and movable part; or (2) as out-of-plane capacitance intended to generate torsional motions of the movable comb part out of the plane of the static part [1], [2]. Mixed designs have also been suggested in the literature [3]. The in-plane interdigitated form is extremely popular as a comb drive and can be used to sustain application-specific stationary drive modes of movable components of the MEMS [4], [5], by loading the comb capacitance with typically sinusoidally varying driving voltages. Other applications include sensing of in-plane lateral distances between components, long-range actuation [3], [6]–[8], microoptics [9] and nanophotonics [10].

One of the predominant aspects of in-plane interdigitated comb drives is the (approximate) linearity of the capacitance over a wide range of displacement, as long as the fingers remain engaged, resulting in an electrostatic drive force almost independent of (lateral) displacement. In this paper we shall be dealing with electric fields on in-plane interdigitated comb drives, in the regime where fingers are deeply engaged; referring to Fig. 1 this means that the overlap region s will be assumed to be much larger than finger width w and finger-to-finger gap d. If, in addition, the finger height h is assumed to be (a few times) larger than w and d, the electric field $\mathbf{E}_1$ between opposite side walls of the fingers can be approximated by standard plate capacitor formulas. On the other hand, the fingers are also sources for electric fringe fields $\mathbf{E}_2$ originating from the finger tips, and fringe fields $\mathbf{E}_3$ emanating from the upper and lower finger surfaces, see Fig. 1. Fringe fields $\mathbf{E}_3$ are the main topic of this paper. Our goal is to provide analytical formulae for $\mathbf{E}_3$ when fingers are deeply engaged. We aim to work to within a degree of simplification and approximation which is comparable to the way the electric field in the interior of a standard plate capacitance is derived.

One motivation for such an investigation could be the desire to quickly evaluate the electrostatic forces acting on the movable part of a comb drive in out-of-plane direction when the fringe fields $\mathbf{E}_3$ below the fingers have a distorted geometry compared to the fields $\mathbf{E}_3$ extending from the upper finger surfaces, or simply become negligible compared to the latter. This situation can occur when a conducting plate or "shield" is placed underneath the comb drive and is loaded with a well-defined voltage; the associated asymmetry in upper and lower fringe fields $\mathbf{E}_3$ then gives rise to a resulting out-of-plane or "levitation" force which can pull the movable comb part away from the shield [11]. In order to evaluate the impact of the levitation forces it is desirable to have reasonably simple analytical expressions for the electric fringe fields $\mathbf{E}_3$ at hand. The objective of this paper is to derive such simple expressions using methods from Potential Theory, and utilizing approximations which will arise from the assumptions stated in the next section.

Previous efforts to analytically determine the electric field ambient to a comb capacitance must be mentioned duly: In [12], electrostatic forces in a comb drive with and without grounded plane underneath have been computed via the principle of virtual work and conformal mapping techniques. The two cases of engaged/disengaged fingers were treated separately, employing approximations based on the assumption that finger width w, gap d and height h be small compared to either the finger overlap s (engaged case) or finger separation (comb parts disengaged). Since the two solutions did not match in the transition region, a linear fit between them had to be provided. – Analytic solutions to electrostatic forces acting in an asymmetric comb drive have been derived in [1], using a potential-theoretical starting point similar to the one given in this paper inasmuch as a reduction of the field geometry to two dimensions was carried out. Results were then derived based on the assumption that the width w of comb fingers is

Hanno Hammer is with the Research and Development Department at SensorDynamics AG, Schloss Eybesfeld 1e, 8403 Graz-Lebring, Austria.

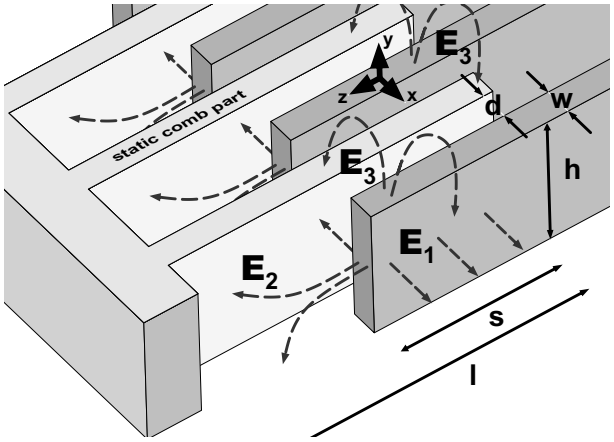

Fig. 1. l: finger length. s: finger overlap. w: finger width. d: finger-finger gap. h: comb height. – Electric fields: Only field lines emanating from movable comb parts are shown. $\mathbf{E}_1$: Field emanating from side walls; $\mathbf{E}_2$: field emanating from finger front faces; $\mathbf{E}_3$: field emanating from upper and lower finger faces. – Triad: Coordinate axes used in computations below.

infinitely small. – The levitation force as a fringe field effect has been thoroughly investigated in [11], where the physical reason for levitation was correctly identified as the asymmetric field geometry due to the presence of a voltage-biased shield underneath the moving fingers; the theoretical treatment of the levitation force has been restricted to a phenomenological formula which was then confirmed experimentally. – In [3], electrostatic forces in a laterally driven comb drive actuator were investigated; the idea of solving Laplace's equation for the electric potential by means of the method of "separation of variables" [13]–[15] was mentioned there but not carried out; the actual field geometry was then determined via Finite Element (FEM) methods.

Our own treatment of fringe fields $\mathbf{E}_3$ makes no effort at being completely rigorous, if that is possible at all. Instead, we focus on a narrow but well-defined case of practical engineering interest, as follows: We analytically compute fringe fields $\mathbf{E}_3$ for the case of a comb capacitance consisting of a stationary and a movable comb part from both of which interleaving fingers are protruding, as shown in Fig. 1. We consider the case of engaged fingers only. It will be assumed that finger width w and finger-to-finger gap d are small compared to both overlap distance s and finger length l. In contrast to [12] we make no assumption that the height h of fingers is small; on the contrary, it will be assumed that fingers have a high aspect ratio, i.e., h is several times the magnitude of both w and d. In contrast to [1] we do take into account a finite width w of the fingers. The plan of the paper then is as follows:

II. Working assumptions. Plan of the paper

In this paper we wish to determine the *upper* $\mathbf{E}_3$ fringe field on a comb capacitance extending into the domain $y \geq 0$ above the fingers, with no conducting surfaces, such as a shield, in the neighbourhood. The fringe field $\mathbf{E}_3$ will be determined from the electrostatic potential which arises as a solution to an appropriately defined Dirichlet problem. In order to formulate a simple Dirichlet problem we shall make use of the following assumptions:

- (A1) The gap d between adjacent fingers shall be small compared to overlap, $d \ll s$;
- (A2) the number N of fingers on the combs shall be large, $N \gg 1$; and
- (A3) the gap d between adjacent fingers shall be small compared to finger height, $d \ll h$.

The plan of the paper is then as follows: In section III we explain how assumptions A1–A3 can be utilized to determine an appropriate domain for a Dirichlet formulation of the electric potential. We demonstrate how symmetries inherent to a problem with many fingers (A2) can be used to determine boundary conditions for the potential on the domain boundary without explicit knowledge of the potential. In section IV we indicate the main steps to solve for the potential and represent the solutions for potential and electric field as infinite series. Section V introduces the truncated version of these series, involving only a finite number of terms. In section VI we compare the series representing potential and electric field components with the results from FEM simulations, discuss discrepancies between the two and address limitations of the approximations made to derive the analytical potential. In section VII we use the analytical result to determine a first approximation to the levitation force that acts on the upper surfaces of movable fingers when a voltage-loaded shield is placed underneath the comb capacitance. In section VIII, this result is used to derive a mean length of electric field lines for the upper $\mathbf{E}_3$ fringe field. Finally, in appendix A we investigate convergence of the series for potential and electric field components and, in the course it, identify singular points in the physics of the problem.

III. Electrostatic Potential as a Solution to a Dirichlet Problem

We work in the coordinate system as picturized in Figs. 1, 2: The coordinate origin is placed such that the width w of a movable finger extends over the interval $-w/2 \leq x \leq w/2$; the upper surface of this finger is located at $y = 0$; and the coordinate origin is located in the centre of the finger overlap region such that the latter covers the range $-s/2 \leq z \leq s/2$.

As stated in the introduction, we shall determine the upper electric fringe field $\mathbf{E}_3$ as the (negative) gradient of the electrostatic potential $\Phi(x, y, z)$ in a domain contained in the half-space $y \geq 0$, i.e. the region above the comb fingers. The domain will be kept as simple as possible by utilizing approximate symmetries obeyed by the potential when conditions A1–A3 are assumed to hold, and will be specified in detail below. In its fullest generality, the potential is a solution to the Poisson equation [13]–[15]

$$\Delta\Phi = -\frac{\rho}{\epsilon_0 \epsilon_r} \quad , \tag{1}$$

where $\Delta = \partial_x^2 + \partial_y^2 + \partial_z^2$ is the Laplace operator, $\rho = \rho(x, y, z)$ is the charge density, ϵ_0 is the electric permittivity of vacuum and ϵ_r is the relative permittivity of the field-carrying domain. In the specified domain $y \geq 0$, no charges are present, hence $\rho = 0$. Furthermore we assume that the domain is filled with

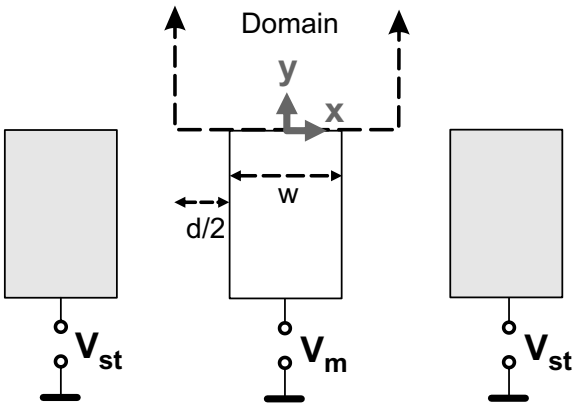

Fig. 2. Cross-section at $z = 0$ through the domain $\mathcal{D}$ in which the electrostatic potential Φ is to be solved for. – V_{st}: Potential on static finger. V_m: Potential on movable finger.

vacuum so that $\epsilon_r = 1$. The potential is uniquely determined only if boundary conditions are supplied: We can either prescribe potential (Dirichlet boundary conditions), electric field (von Neumann b.c.), or mixed boundary conditions on the domain boundary. We shall now argue that the potential is most easily solved for within a Dirichlet formulation of the problem.

When the gap d is small compared to overlap s (A1), the fringe field along the upper surface $y = 0$ will vary weakly with z, as long as z takes values within the interior of the range $-s/2 < z < s/2$; only near the boundaries $z = \pm s/2$ will there be significant deviations from the field geometry within. We thus have approximate z-symmetry of the potential and hence can approximate the fringe field by its geometry at the centre plane $z = 0$. This implies for the potential that

$$\Phi(x, y, z) = \Phi(x, y) \quad . \tag{2}$$

We have thus reduced the problem to two dimensions only.

In the absence of other conducting bodies the potential is defined only up to an arbitrary constant, or, put in another way, only the potential difference $\Phi_0 = V_m - V_{st}$ is physically relevant (V_m, V_{st} is the potential on moving/static fingers). We can therefore redefine the potentials according to

$$\begin{aligned} V_m &\to \Phi_0/2 \quad , \\ V_{st} &\to -\Phi_0/2 \quad , \end{aligned} \tag{3}$$

without changing the physics of the problem. Furthermore, a large number N of fingers (A2) implies the following "swap symmetry": the physics of the problem must be invariant under translations along x by $\pm(w + d)$, followed by swapping potentials, $V_{st} \to V_m$, $V_m \to V_{st}$. The symmetry inherent in A2 together with swap symmetry and (3) then imply that the potential must satisfy

$$\Phi\Big(x \pm (w + d), y\Big) = -\Phi\Big(x, y\Big) \quad . \tag{4}$$

Due to this symmetry we need to solve (1) only within the domain $\mathcal{D}$ defined by the interval $x = -(w + d)/2$ to $x = +(w + d)/2$ and $0 \le y < +\infty$. An xy cross-section through the domain $\mathcal{D}$ at $z = 0$ is picturized in Fig. 2.

To fully specify the Dirichlet problem we now must predetermine the values the potential takes at the boundary of $\mathcal{D}$. It is intuitively clear – and can be easily derived from (4) – that the surfaces $x = \pm\frac{w+d}{2}$ are potential surfaces where $\Phi = 0$,

$$\Phi\left(\pm\frac{w + d}{2}, y\right) = 0 \quad . \tag{5}$$

Next, since there are no charges placed at $y \to +\infty$, the potential must be constant there; hence, by continuity with $\Phi(x = \pm\frac{w+d}{2}, y \to \infty)$ we must have that

$$\lim_{y\to\infty} \Phi(x, y) = 0 \quad . \tag{6}$$

On the opposite boundary, the potential at $y = 0$ is equal to

$$\Phi(x, 0) = \Phi_0/2 \quad , \quad \text{for} \quad -\frac{w}{2} \le x \le \frac{w}{2} \quad , \tag{7}$$

i.e., within the upper finger area.

Finally we need to prescribe values for the potential at height $y = 0$ but within the gap, i.e. for $\frac{w}{2} \le x \le \frac{w+d}{2}$ and $-\frac{w+d}{2} \le x \le -\frac{w}{2}$. It is here where we need assumption A3: When the gap d is small compared to the height h of the fingers, the geometry of the electric field within the gap, e.g. for $\frac{w}{2} \le x \le \frac{w+d}{2}$ at $y = 0$, should closely resemble the homogeneous field seen in the interior of a large plate capacitance, i.e., featuring only an x component which is equal in magnitude to the potential difference divided by the gap size, Φ_0/d. This suggests that, on the surface $y = 0$ within the gap, the potential varies approximately linearly with x between its extreme value $\Phi_0/2$ on the upper surface of the movable finger and $\Phi = 0$ in the middle of the gap, at $x = \pm\frac{w+d}{2}$. Hence the last boundary condition on Φ will be taken to be

$$\Phi(x, 0) = \begin{cases} \frac{\Phi_0}{2} & , \quad -\frac{w}{2} \le x \le \frac{w}{2} \\ -\frac{\Phi_0}{d}x + \frac{\Phi_0}{2}\left(1 + \frac{w}{d}\right) & , \quad \frac{w}{2} \le x \le \frac{w+d}{2} \\ \Phi(-x, 0) & , \quad -\frac{w+d}{2} \le x \le -\frac{w}{2} \end{cases} . \tag{8}$$

IV. Solution to the fully specified Dirichlet problem

We have now fully specified the (two-dimensional) potential $\Phi(x, y)$ along the boundaries of the domain $\mathcal{D}$ introduced in section III. Since there are no charges in the interior of this domain it is seen from eq. (1) that we are left to solve the two-dimensional Laplace equation

$$\Delta\Phi(x, y) = \left(\frac{\partial^2}{\partial x^2} + \frac{\partial^2}{\partial y^2}\right)\Phi(x, y) = 0 \tag{9}$$

in $\mathcal{D}$, subject to boundary conditions (5, 6, 8). The rectangular geometry of the problem suggests a factorized trial solution

$$\Phi(x, y) = \Phi_1(x)\Phi_2(y) \quad . \tag{10}$$

As expounded in all standard texts on the solution of Laplace's equation, eq. (9) then implies that Φ_1, Φ_2 obey

$$\frac{\partial^2\Phi_1}{\partial x^2} = c\Phi_1 \quad , \tag{11a}$$

$$\frac{\partial^2\Phi_2}{\partial y^2} = -c\Phi_2 \quad , \tag{11b}$$

where c is an as yet arbitrary real constant. From (11a) we see that candidates for Φ_1 are trigonometric and/or hyperbolic sines and cosines. Our choice of coordinate system is such as to make the potential symmetric, $\Phi(x) = \Phi(-x)$, hence only trigonometric or hyperbolic cosines are eligible. Since (5) must hold, hyperbolic cosines must be discarded. Thus, functions Φ_1 will be trigonometric cosines $\cos ax$, where a is chosen so as to make Φ_1 vanish at $x = \pm\frac{w+d}{2}$. This gives

$$\begin{aligned} \Phi_{1,k}(x) &= \cos\left(a_k x\right) \quad , \\ a_k &= \left(2k+1\right)\frac{\pi}{w+d} \quad , \quad k \in \mathbb{N}_0 \quad . \end{aligned} \tag{12}$$

Functions Φ_2 then must satisfy eq. (11b) with $c = -a^2$ negative. That leaves only hyperbolic functions or, equivalently, basis functions $\exp(\pm ay)$ for Φ_2. The positive sign is not applicable as we cannot satisfy boundary condition (6) with this choice. Thus, the base function $\Phi_{2,k}$ associated with a given choice of a_k is

$$\Phi_{2,k}(y) = e^{-a_k y} \quad , \tag{13}$$

and a solution of (9) satisfying the first two boundary conditions (5, 6) is given by

$$\Phi_k(x,y) = A_k \cos\left(a_k x\right) e^{-a_k y} \quad , \tag{14}$$

with as yet unspecified real coefficient A_k. By linearity of Laplace's equation, the full solution is a superposition

$$\Phi(x,y) = \sum_{k=0}^{\infty} A_k \cos\left(a_k x\right) e^{-a_k y} \tag{15}$$

of terms (14) with A_k chosen so as to satisfy the last boundary condition

$$\Phi(x,0) = \sum_{k=0}^{\infty} A_k \cos\left(a_k x\right) \quad , \tag{16}$$

where boundary values $\Phi(x,0)$ are specified in (8). It is seen that A_k are the coefficients of $\Phi(x,0)$ in a Fourier cosine expansion on the domain $-\frac{w+d}{2} \le x \le \frac{w+d}{2}$. They can therefore be determined using standard methods from Fourier Analysis, resulting in

$$\begin{aligned} A_k &= \frac{4\Phi_0}{d\left(w+d\right)a_k^2}\cos\left(a_k\frac{w}{2}\right) = \\ &= \frac{4\Phi_0}{\pi^2\left(2k+1\right)^2}\frac{w+d}{d}\cos\left[\left(2k+1\right)\frac{\pi}{2}\frac{w}{w+d}\right] \quad . \end{aligned} \tag{17}$$

This determines the potential as

$$\begin{aligned} \Phi(x,y) = &\sum_{k=0}^{\infty}\frac{4\Phi_0}{\pi^2\left(2k+1\right)^2}\frac{w+d}{d}\times \\ &\times\cos\left[\left(2k+1\right)\frac{\pi}{2}\frac{w}{w+d}\right]\cos\left[\left(2k+1\right)\frac{\pi x}{w+d}\right]\times \\ &\times\exp\left[-\left(2k+1\right)\frac{\pi y}{w+d}\right] \quad . \end{aligned} \tag{18}$$

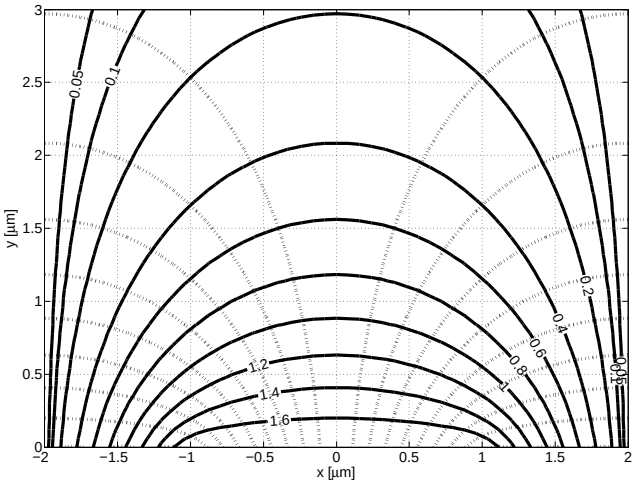

Fig. 3. Potential surfaces (solid -) and electric field lines (dashed ··) of the truncated analytical potential eq. (20), in the region $-2 \le x \le 2$ μm and $0 \le y \le 3$ μm, for $N = 10$, finger width $w = 2$ μm, finger gap $d = 2$ μm, and potential drop $\Phi_0 = 3.6$ V. Labels indicate potential values at the given potential surface. The finger ranges between $x = \pm 1$ μm. Close to the finger surface, at $y = 0$, the potential approaches $+\Phi_0/2 = 1.8$ V.

The components of electric field strength are given by

$$E_x = -\frac{\partial\Phi}{\partial x} = \sum_{k=0}^{\infty} A_k a_k \sin\Big(a_k x\Big) e^{-a_k y} \quad , \tag{19a}$$

$$E_y = -\frac{\partial\Phi}{\partial y} = \sum_{k=0}^{\infty} A_k a_k \cos\Big(a_k x\Big) e^{-a_k y} \quad . \tag{19b}$$

V. Finite series truncation of the potential

In practise we will ever only deal with a truncation of the infinite series (18), containing only a finite number $N+1$ of terms,

$$\Phi(x,y) = \sum_{k=0}^{N} A_k \cos\left(a_k x\right) e^{-a_k y} \quad . \tag{20}$$

As will be shown in the next chapter, the accuracy of a truncation involving only few ($\approx$ 3-4) terms is still very acceptable in regions located not too close to charged surfaces, and mostly deteriorates in the neighbourhood of the finger edges at $x = \pm\frac{w}{2}$.

In Fig. 3 we plot potential surfaces and electric field lines of (20), truncated at $N = 10$, with finger width $w = 2$ μm, finger gap $d = 2$ μm, and potential drop $\Phi_0 = 3.6$ V between static and movable comb.

VI. Comparison of analytical model with FEM Simulations

In this section we present results from electrostatic FEM simulations of the comb capacitance which will be compared with the truncated analytical model (20). It will be demonstrated that, in general, the truncated series provides good accuracy, except for regions close to the edges of the fingers.

In Figs. 4–6 we compare the potential, horizontal electric field component E_x, and vertical electric field component E_y obtained from a FEM analysis with the respective quantities

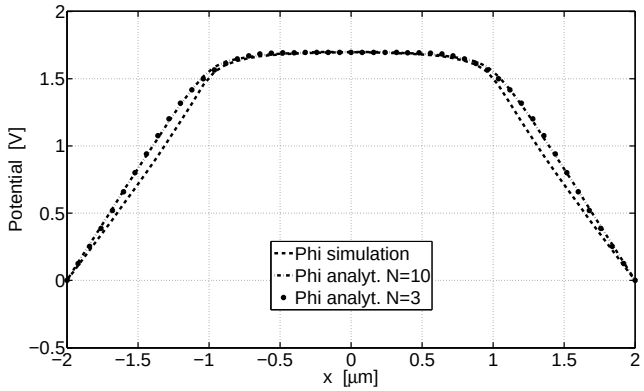

Fig. 4. Plot of potential $\Phi(x, y)$ versus x over the whole x-range of the domain $\mathcal{D}$, at height $y = 0.1$ μm above finger. Dashed: FEM simulation with spatial resolution of 0.2 μm. Dot-dashed: Analytical model truncated at $N = 10$. Circles: Analytical model truncated at $N = 3$.

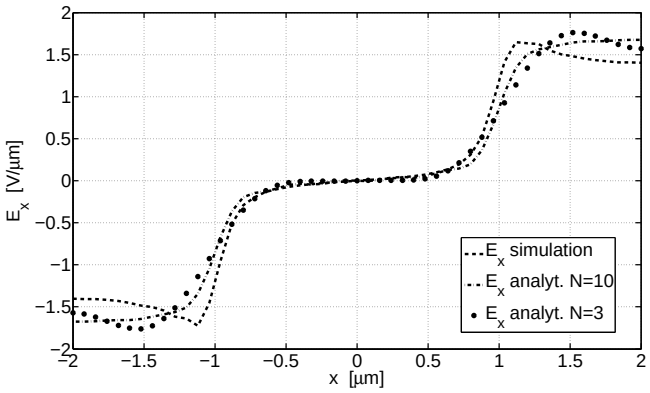

Fig. 5. Plot of horizontal electric field component E_x versus x over the whole x-range of the domain $\mathcal{D}$, at height $y = 0.1$ μm above finger. Dashed: FEM simulation with spatial resolution of 0.2 μm. Dot-dashed: Analytical model truncated at $N = 10$. Circles: Analytical model truncated at $N = 3$.

derived from truncated formula (20) and the truncated versions of 19a, 19b, for $N = 3$ and $N = 10$. The reported quantities refer to a path parallel to the upper finger surface, extending along the x-direction over the whole range $-2 \leq x \leq 2$ μm of the Dirichlet domain, and located at $y = 0.1$ μm above the surface. The path constitutes the x-axis on the plots. The FEM model has a spatial resolution of ≈ 0.2 μm, i.e., potential values are reported at spatial intervals of 0.2 μm and then linearly interpolated to produce a continuous plot.

Within the range of the upper finger surface $|x| \leq 1$, the analytical model coincides with simulation quite satisfactorily, even for small values of N, and irrespective of the location above the finger surface. On the other hand, within the gap, i.e., for $w/2 \leq |x| \leq (w + d)/2$, the analytical values for the electric potential are higher than the simulated ones. This results in a different slope of the analytical potential with respect to x, and hence analytical E_x slightly differs from the simulated one. We think that the reason lies with (8): Amongst all boundary conditions, this one involves the most severe approximation to the real situation, or, to put it another

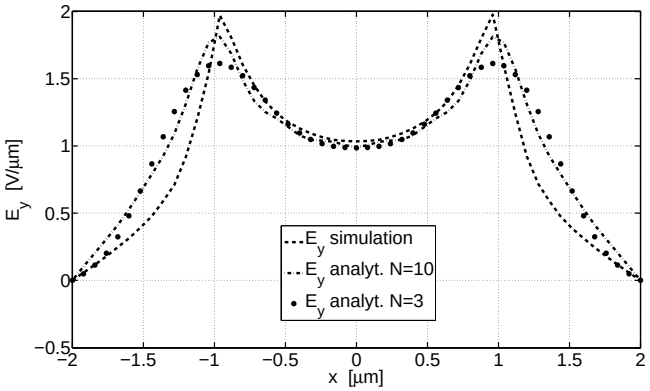

Fig. 6. Plot of vertical electric field component E_y versus x over the whole x-range of the domain $\mathcal{D}$, at height $y = 0.1$ μm above finger. Dashed: FEM simulation with spatial resolution of 0.2 μm. Dot-dashed: Analytical model truncated at $N = 10$. Circles: Analytical model truncated at $N = 3$.

way: the real potential at the upper rim of the gap region *does* deviate from the strictly linear behaviour that was assumed in (8). This may be confirmed by direct visual inspection of, e.g., Fig. 4 where the FEM result shows a slight deviation (towards lower values) of the potential variation from linear decrease.

VII. Fringe fields and levitation forces

In a real MEMS sensor, various reasons may make it necessary to situate the combs above a conducting plate which is kept on the same potential as, say, the movable part of the comb capacitance and which may be called "shield" in what follows. As a consequence, the fringe field geometry $\mathbf{E}_3$ is no longer symmetric above and below the comb: For, field lines ending on the bottom surface of the static fingers will originate both from the bottom of the movable fingers and from the shield, whereas field lines extending from the top surfaces of the movable fingers upwards will mostly end on adjacent static fingers, see Fig. 7. The resulting asymmetry in $\mathbf{E}_3$-field geometry creates an imbalance in electrostatic forces acting on the surface charges of the movable comb part along the y direction. For the voltage load as described, namely, shield potential = movable comb potential, this resulting force is always directed upwards (along positive y) and hence is appropriately called *levitation force* [11].

We are mostly interested in the case where the shield is placed so narrowly underneath the comb that most of the electric flux terminating on the lower surfaces of the static fingers comes from the shield. This means that there is negligible electric flux emanating from the lower surface of the movable fingers, and hence the lower $\mathbf{E}_3$ fringe field on the movable finger is basically zero. In this case, the levitation force on the movable finger is generated by the upper $\mathbf{E}_3$ fringe field only. We now derive the levitation force under this approximation:

The forces on fingers arise from electric fields acting on the surface charges accumulating on the finger surfaces. Thus, the vertical force component F_y acting on the upper surface of a

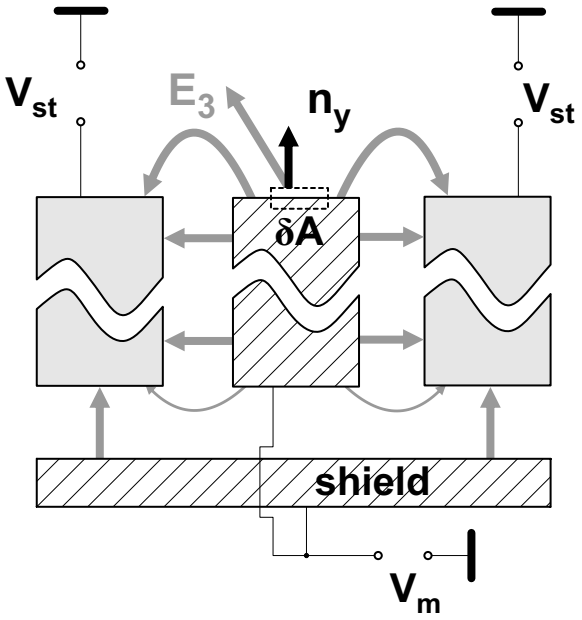

Fig. 7. Cross section through comb fingers, with shield underneath. Middle finger: movable, is kept on same potential V_m as shield. Outer fingers: static, are kept on potential V_{st}. Grey arrows: Electric fields $\mathbf{E}_3$, and $\mathbf{E}_1$ (within gap). As there is no potential difference between movable finger and shield, fringe field $\mathbf{E}_3$ is strong on upper face of movable finger but weak on lower face. This imbalance generates levitation force. – $\mathbf{n}_y$: Unit vector normal to upper finger surface. Shown is a small rectangular box with face area δA and infinitesimal height, for determination of surface charges via Gauß' law.

movable finger is given by

$$F_y = \int_S dA\, \sigma E_y \quad , \tag{21}$$

where $S = sw$ is the total area of the upper surface of the movable finger within the overlap region, σ is the surface charge density on the finger, and E_y is obtained from (19b). The surface charge density can be determined from the vertical component E_y of the fringe electric field $\mathbf{E}_3$ as follows: We integrate *Gauß' law*

$$\nabla \bullet \mathbf{D} = \rho \tag{22}$$

over a shallow "pillbox"-shaped volume with infinitesimal height δh and "small" area δA, which intersects the upper surface of the movable finger as seen in Fig. 7, and use Gauß' theorem. This gives

$$\oint_S dA\, \mathbf{n} \bullet \mathbf{D} = \int_{V(S)} dV\, \rho = \delta Q \quad , \tag{23}$$

where S is the boundary of the pillbox, $V(S)$ is its volume, and δQ is the total charge contained in it. Inside the conductor the displacement field is zero (as well as the electric field). The only nonvanishing component is therefore the normal component

$$\mathbf{n}_y \bullet \mathbf{D} = D_y = \epsilon_0 E_y \tag{24}$$

on the outer surface of the conductor, where in the last equation we have made use of the fact that the space ambient

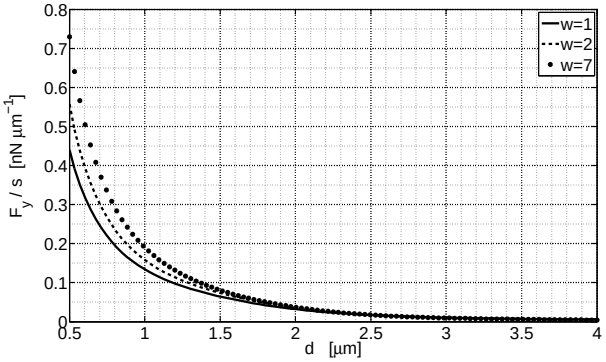

Fig. 8. Electrostatic "levitation" force from upper fringe field $\mathbf{E}_3$ per unit overlap, in nano-Newton per μm, for three different finger widths $w = 1, 2, 7$ μm, with gap d varying between 0.5 and 4 μm.

to the fingers is filled with vacuum, hence $\mathbf{D} = \epsilon_0 \mathbf{E}$ there. The last two equations say that

$$\epsilon_0 E_y \delta A = \delta Q \quad . \tag{25}$$

On the other hand, the total charge contained in the "pillbox" is equal to

$$\delta Q = \sigma \delta A \quad , \tag{26}$$

thus eqs. (25, 26) imply that

$$\sigma(x) = \epsilon_0 E_y(x, 0) \quad . \tag{27}$$

Combining the last result with (21) we obtain for the levitation force per finger

$$\begin{aligned} F_y &= \int_{x=-w/2}^{w/2} dx \int_{z=-s/2}^{s/2} dz\, \sigma\, E_y = \\ &= s\epsilon_0 \int_{-w/2}^{w/2} dx\, E_y^2(x, 0) \quad . \end{aligned} \tag{28}$$

On inserting truncated formula (19b) into (28) and performing the x-integration we obtain

$$\begin{aligned} F_y &= \frac{sw\epsilon_0}{2} \sum_{k,l=0}^{N_{\text{trunc}}} A_k A_l a_k a_l \times \\ &\times \left\{ H\left((a_k + a_l)\frac{w}{2}\right) + H\left((a_k - a_l)\frac{w}{2}\right) \right\} \quad , \\ H(x) &= \frac{\sin x}{x} \quad . \end{aligned} \tag{29}$$

Since, in our approximation, the levitation force is proportional to overlap, it makes sense to compare the force F_y/s per unit overlap s versus variable gap d and/or finger width w. This is done in Fig. 8 for finger widths $w = 1, 2, 7$ μm, and gap d varying between 0.5 and 4 μm.

VIII. Mean length of fringe field lines

We can use formula (29) to derive a mean length of field lines for fringe fields $\mathbf{E}_3$ on the upper finger surfaces, by comparing (29) with the force acting on a plate capacitance. The force on one plate of a plate capacitance with area A, gap

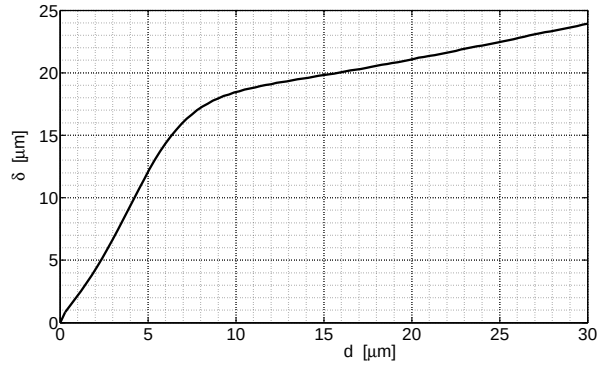

Fig. 9. Mean length of upper $\mathbf{E}_3$ fringe field lines δ [μm] between adjacent fingers, vs. d, for $0 \leq d \leq 30$ μm. It is seen that δ has two quasi-linear regimes connected at $d \approx 8$.

d, voltage load Φ_0, absolute value of total charge on one plate Q, and interior electric field strength E is

$$F = Q\frac{E}{2} = \epsilon_0 \frac{A\Phi_0^2}{2d^2} \quad . \tag{30}$$

Eq. (29) can now be put in a similar form,

$$F_y = \epsilon_0 \frac{sw\Phi_0^2}{2\delta^2} \quad , \tag{31}$$

where sw is the upper area of one finger, being the equivalent of the plate area in a plate capacitance; and

$$\delta = \frac{d}{\sqrt{G\left(\frac{d}{w}\right)}} = \frac{d}{\sqrt{G(p)}} \quad , \quad p \equiv \frac{d}{w} > 0$$

$$G(p) \equiv \left(\frac{4}{\pi}\right)^2 \sum_{k,l=0}^{\infty} \frac{\cos\left((2k+1)\frac{\pi}{2}\frac{1}{1+p}\right)}{2k+1} \times$$

$$\times \frac{\cos\left((2l+1)\frac{\pi}{2}\frac{1}{1+p}\right)}{2l+1} \times$$

$$\times \left\{ H\Big(\frac{\pi}{1+p}(k+l+1)\Big) + H\Big(\frac{\pi}{1+p}(k-l)\Big) \right\} \quad . \tag{32}$$

It is seen that δ represents an effective gap size, or, equivalently, a *mean length of upper* $\mathbf{E}_3$ *fringe field lines* starting at the moving finger and ending – half left, half right – on the upper surfaces of adjacent static fingers, as in Fig. 1. For a finger width $w = 2$ μm we vary the gap d between 0 and 30 μm and plot $\delta(d)$ versus d in Fig. 9. It is seen that this function basically has two linear regimes meeting at $d \approx 8$.

IX. Summary

Electrostatic fringe fields emanating from the upper surfaces of movable comb fingers have been introduced within the context of MEMS comb capacitances. Three assumptions on comb geometry have been introduced by means of which the problem of determining the electrostatic potential associated with $\mathbf{E}_3$ fringe fields could be solved within an appropriately defined Dirichlet domain. It was shown that, using symmetries inherent to the comb geometry, a simple problem domain could be introduced such that boundary values for the potential were found without explicit knowledge of the potential. The fully specified Dirichlet problem then could be solved for explicitly. The accuracy of analytical results has been compared with results from FEM simulations of potentials and field strength components. It has been demonstrated that, apart from edge regions, even series truncations involving only very few terms compare very well with the FEM simulation results. Analytic results for vertical electric field components on the upper finger surfaces were used to derive the electrostatic force acting on these faces. It was argued that, in the presence of a conducting surface closely underneath the combs which is loaded with the same potential as the movable fingers, this force could be used as a first approximation for estimating the full levitation force on the movable comb parts. From the same result we derived a mean length of fringe electric field lines, pertaining to the $\mathbf{E}_3$ field emanating from the upper finger surfaces. – In the appendix, convergence properties of the series for potentials and electric field components are discussed. It is demonstrated that, in the interior of the domain, the series for potential and electric field components converge in the absolute sense. At the singular points defined by finger edges, the series for horizontal electric field component converges towards the mean value of left and right limit of the real physical field strength there, as is to be expected from a Fourier-like series, while the series for the vertical component apparently diverges, in line with physical intuition of electric fields in edge regions.

Appendix
Discussion of convergence and singular points

The series (18) for the potential converges everywhere in the absolute sense. This can be seen as follows: The modulus of each term in the series can be estimated upwards according to

$$\left| \frac{4\Phi_0}{\pi^2(2k+1)^2} \frac{w+d}{d} \times \cos\left[(2k+1)\frac{\pi}{2}\frac{w}{w+d}\right] \times \right.$$
$$\left. \times \cos\left[(2k+1)\frac{\pi}{w+d}x\right] \exp\left[-(2k+1)\frac{\pi y}{w+d}\right] \right| \leq$$
$$\leq \frac{4\Phi_0}{\pi^2(2k+1)^2} \frac{w+d}{d} \quad , \tag{33}$$

where we have replaced $|\cos|$ and the exponential by one. The series that can be built from the remaining term in the last row is proportional to

$$\sum_{k=0}^{\infty} \frac{1}{(2k+1)^2} < \sum_{n=1}^{\infty} \frac{1}{n^2} = \frac{\pi^2}{6} \quad , \tag{34}$$

and hence converges in the absolute sense. Thus, the series made from terms given in the first row of (33) converges, which implies that (9) converges in the absolute sense, and independently of the values of x, y within the domain $\mathcal{D}$.

For the field strength the situation is more complicated. For $y > 0$ the exponential in the series expansions (19) guarantees absolute convergence: For, let

$$q \equiv \exp\left(-\frac{2\pi y}{w+d}\right) < 1 \quad \text{for } y > 0 \quad , \tag{35}$$

then (19a) may be written in the form

$$\begin{aligned} E_x = \frac{4\Phi_0}{d\pi} \exp\left(-\frac{\pi y}{w+d}\right) \times \\ \times \sum_{k=0}^{\infty} \frac{1}{2k+1} \cos\left(a_k \frac{w}{2}\right) \sin\left(a_k x\right) \times q^k \quad . \end{aligned} \tag{36}$$

To obtain E_y we only need to replace $\sin(a_k x)$ by $\cos(a_k x)$ in the last formula. But the series on the right-hand side of (36) converges in the absolute sense, since

$$\left| \frac{1}{2k+1} \cos\left(a_k \frac{w}{2}\right) \sin\left(a_k x\right) \times q^k \right| \leq \frac{1}{2k+1} q^k < q^k \quad , \tag{37}$$

and thus has the geometric series

$$\sum_{k=0}^{\infty} q^k = \frac{1}{1-q} \tag{38}$$

as a majorant, which converges due to $q < 1$. Thus, series (19) converge in the absolute sense whenever $y > 0$.

At $y = 0$ the convergence-enforcing property of the exponential term no longer exists; the series (19) then converge except for the two singular points at $x = \pm\frac{w}{2}$, but not in the sense of absolute convergence. At the singular points, the field strengths behave like this:

The actual, physical x-component of the field strength is not defined at $(\pm\frac{w}{2}, 0)$. However, there exist the left and right limits

$$\begin{aligned} \lim_{\epsilon \to 0} E_x\left(\frac{w}{2} - \epsilon, 0\right) = 0 \quad , \\ \lim_{\epsilon \to 0} E_x\left(\frac{w}{2} + \epsilon, 0\right) = \frac{\Phi_0}{d} \end{aligned} \tag{39}$$

at the right edge $(\frac{w}{2}, 0)$, with similar expressions for the left edge. The series (19a) at this point then exhibits the well-known behaviour of Fourier series to converge at discontinuities towards the mean value of the left and right limit of the function at this point. Indeed, for $\Phi_0 = 3.6$ V and $d = 2$ μm, the x-component of the field strength inside the gap is approximately equal to $\Phi_0/d = 1.8$, but, as numerical tests confirm, the series (19a) converges towards a value of 0.9, i.e., the mean value of the two expressions in (39).

The y-component E_y of the electric field strength at the singular points $(\pm\frac{w}{2}, 0)$ is also not well-defined. The series (19b) at $(\frac{w}{2}, 0)$ is equal to

$$E_y\left(\frac{w}{2}, 0\right) = \frac{4\Phi_0}{d\pi} \sum_{k=0}^{\infty} \frac{\cos^2\left(a_k \frac{w}{2}\right)}{2k+1} \quad , \tag{40}$$

which we suspect to diverge. This is confirmed by numerical summations of the last formula. It is also in line with physical intuition: At the edge region the electric field should not be well-defined due to the infinite curvature radius of the edge; but it were so, if both series in (19) would converge properly there.

REFERENCES

[1] J.-L. Yeh, C.-Y. Hui, and N. Tien, "Electrostatic model for an asymmetric combdrive," *Microelectromechanical Systems, Journal of*, vol. 9, no. 1, pp. 126–135, Mar 2000.

[2] A. Lee, C. McConaghy, G. Sommargren, P. Krulevitch, and E. Campbell, "Vertical-actuated electrostatic comb drive with in situ capacitive position correction for application in phase shifting diffraction interferometry," *Microelectromechanical Systems, Journal of*, vol. 12, no. 6, pp. 960–971, Dec. 2003.

[3] T. Kuendiger, G. Howard, P. Mokrian, M. Ahmadi, and W. Miller, "Design and analysis of planar and lattice electrostatic comb drive actuators," *IEEE-NEWCAS Conference, 2005. The 3rd International*, pp. 151–154, June 2005.

[4] A. Shkel, C. Acar, and C. Painter, "Two types of micromachined vibratory gyroscopes," 30 2005-Nov. 3 2005, pp. 6 pp.–.

[5] W. Geiger, B. Folkmer, U. Sobe, H. Sandmaier, and W. Lang, "New designs of micromachined vibrating rate gyroscopes with decoupled oscillation modes," *Solid State Sensors and Actuators, 1997. TRANSDUCERS '97 Chicago., 1997 International Conference on*, vol. 2, pp. 1129–1132 vol.2, Jun 1997.

[6] J. Clark, "Modeling a monolithic comb drive for large-deflection multi-dof microtransduction," July 2008, pp. 203–207.

[7] A. Selvakumar and K. Najafi, "Vertical comb array microactuators," *Microelectromechanical Systems, Journal of*, vol. 12, no. 4, pp. 440–449, Aug. 2003.

[8] C. Lee, S. Han, and N. MacDonald, "Single crystal silicon (scs) xy-stage fabricated by drie and ir alignment," Jan 2000, pp. 28–33.

[9] M.-H. Kiang, O. Solgaard, K. Lau, and R. Muller, "Electrostatic combdrive-actuated micromirrors for laser-beam scanning and positioning," *Microelectromechanical Systems, Journal of*, vol. 7, no. 1, pp. 27–37, Mar 1998.

[10] S. Waldis, S. Weber, W. Noell, J. Extermann, D. Kiselev, L. Bonacina, J.-P. Wolf, and N. de Rooij, "Large linear micromirror array for uv femtosecond laser pulse shaping," Aug. 2008, pp. 39–40.

[11] W. Tang, M. Lim, and R. Howe, "Electrostatic comb drive levitation and control method," *Microelectromechanical Systems, Journal of*, vol. 1, no. 4, pp. 170–178, Dec 1992.

[12] W. Johnson and L. Warne, "Electrophysics of micromechanical comb actuators," *Microelectromechanical Systems, Journal of*, vol. 4, no. 1, pp. 49–59, Mar 1995.

[13] R. J. Jelitto, *Theoretische Physik III. Elektrodynamik*, 2nd ed. Wiesbaden: Aula-Verlag GmbH, 1987.

[14] J. D. Jackson, *Classical Electrodynamics*, 3rd ed. New York: John Wiley, 1999.

[15] W. K. H. Panofsky and M. Phillips, *Classical Electricity And Magnetism*, 2nd ed. Reading: Addison-Wesley, 1962.